Ferroelectric and antiferroelectric coupling in superlattices of paraelectric perovskites at room temperature

Hans M. Christen,[1] Eliot D. Specht,[2] Sherwood S. Silliman,[3,*] and K. S. Harshavardhan[3]

[1]*Oak Ridge National Laboratory, Condensed Matter Sciences Division, Oak Ridge, Tennessee 37831-6056, USA*
[2]*Oak Ridge National Laboratory, Metals and Ceramics Division, Oak Ridge, Tennessee 37831-6118, USA*
[3]*Neocera, Inc., 10000 Virginia Manor Road, Beltsville, Maryland 20705, USA*

Results from dielectric and structural measurements on epitaxial $SrTiO_3$/$BaZrO_3$ superlattices reveal properties that cannot be explained simply in terms of those measured on single films of the constituent materials. For large superlattice periodicities (20/20 and 38/38 structures—i.e., samples in which each $SrTiO_3$ and $BaZrO_3$ layer are 20 or 38 unit cells thick, respectively), the capacitance-voltage curves indicate room-temperature ferroelectricity. For smaller periodicities (7/7 and 15/15), antiferroelectric-type behavior is observed, suggesting strong coupling between individual polar layers. This is consistent with recent second-harmonic generation results [A.Q. Jiang *et al.*, J. Appl. Phys. **93**, 1180 (2003)] of ordering in $SrTiO_3$/$BaTiO_3$ superlattices. However, both constituents of the structures investigated here are paraelectric. Strain-induced room-temperature ferroelectricity in $SrTiO_3$ and distance-dependent coupling between these layers are proposed as mechanisms leading to the observed behavior.

The periodic stacking of epitaxial perovskite films—and thus the formation of artificial superlattice structures—allows us to intimately couple dissimilar materials and to observe emerging physical properties that are not necessarily a simple combination of those found in the constituent materials. Motivated by both the technological interest in ferro-electrics for device applications and the quite good understanding of these materials' intriguing properties, structures consisting of paraelectric and ferroelectric layers have received considerable attention. Here we report on the observation of ferroelectric and antiferroelectric properties in structures consisting entirely of paraelectric constituents and show that the data are compatible with an interpretation of strain-induced ferroelectricity at room temperature and spacing-dependent coupling between such layer.

Periodic heterostructures consisting of paraelectric and ferroelectric perovskite titanate or niobate layers have been studied in detail before.[1–5] In the case of $KTaO_3$/$KNbO_3$ superlattices, for example, it was observed that below a critical layer spacing, the structural phase transition occurs at the same temperature as that of the alloy,[6,7] but the local structure remains distinctively different from that of the solid solution.[8] Furthermore, dielectric measurements show evidence of antiferroelectricity in 1/1 superlattices.[9]

$SrTiO_3$ is typically described as a quantum paraelectric—i.e., a material in which ferroelectricity would occur at low temperature if it were not for the quantum fluctuations. The lattice is easily be distorted by impurities (such as Ca or Ba on the Sr site), leading to local polar clusters or ferroelectric states. In addition, the dielectric constant is strongly pressure sensitive,[10–12] and a transition to a ferroelectric state at low temperature can be induced by uniaxial stress.[13,14]

More recently, a careful treatment of $SrTiO_3$ films in the presence of misfit strains (resulting from film/substrate interactions) in the framework of the Landau-Ginsburg-Devonshire theory has led to a rather complete description of ferroelectricity in these layers.[15] Room-temperature ferro-

electricity is predicted for large strains of about 0.015, but has not been confirmed experimentally.

Epitaxial superlattices provide the ideal platform to probe the effects of such large misfit strains on $SrTiO_3$. According to a recent report,[16] second-harmonic generation data show that $SrTiO_3$ exhibits a polar state at room temperature in $SrTiO_3$/$BaTiO_3$ superlattices if the $SrTiO_3$ layer thickness falls below 30 unit cells (i.e., 30/30 superlattices). Interestingly, "antidipole patterns" are observed in superlattices with unit cells below 10/10, corresponding to antiferroelectric ordering of the structure.

Dielectric measurements can shed light on the properties of such materials; however, these experiments probe the entire structure, and the properties of a material that is not ferroelectric in its relaxed state may be partially or completely masked by the ferroelectric constituent of the superlattice. In order to circumvent this difficulty, we performed dielectric measurements on superlattices of $SrTiO_3$ and $BaZrO_3$. Both of these materials are cubic ($Pm\bar{3}m$) and paraelectric at room temperature. Our data are consistent with an interpretation (motivated by the above-mentioned study of the related $SrTiO_3$/$BaTiO_3$ structures) of a polar state in $SrTiO_3$ (and/or in $BaZrO_3$) having long-range (inter-layer) order of ferroelectric or antiferroelectric nature depending on the stacking periodicity [ferroelectricity for (20/20) and (38/38) structures, antiferroelectricity for (15/15) and (7/7) structures].

Epitaxial films and superlattices were grown onto $LaAlO_3$ substrates by pulsed laser deposition (PLD) under standard growth conditions (KrF radiation, 2 J/cm^2 at 10 Hz, 200 mTorr oxygen background, and substrates mounted with silver paint to a plate kept at 780 °C). Single-phase ceramic targets were used, and all films were grown with a total thickness of 500 nm.

The superlattices were first characterized by x-ray diffraction. As shown in Fig. 1, satellite peaks are clearly observed
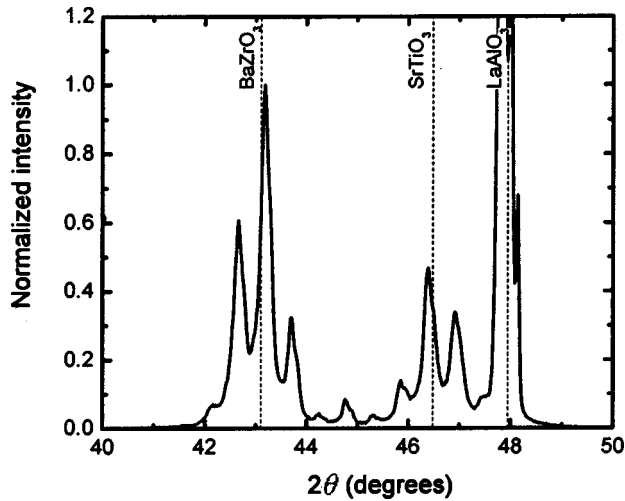
FIG. 1. Normal x-ray θ-2θ scan for a superlattice consisting of BaZrO$_3$ and SrTiO$_3$ layers on a LaAlO$_3$ substrates. From the spacing of the satellite peaks, the periodicity of the structure ($\Lambda = 180$ Å) can be determined.

in normal θ-2θ scans (using a Rigaku two-circle diffractometer) and allow us to determine the periodicity of the structure accurately. Profilometry measurements on single BaZrO$_3$ and SrTiO$_3$ films indicate that the growth rates are identical ($\pm 5\%$) for the two materials; thus, the thickness of each constituent layer is half of the superlattice periodicity.

For the samples with larger periodicity, x-ray diffraction allowed us to determine the in-plane and out-of-plane lattice parameters of both constituents. Out-of-plane measurements were made with a four-circle diffractometer, using Cu $K\alpha$ radiation, and a sagitally focusing focusing graphite monochromator. Reflections were broad, indicating that the layers were incoherent. Measuring the Bragg angle for the (110), (200), (220), (101), (211), (112), and (202) peaks on a (20/20) superlattice shows that the films are strongly strained. Table I shows the results for each material's lattice parameter.

Obviously, the strain in these films results not from clamping to the substrate, but from the interaction between the SrTiO$_3$ and BaZrO$_3$: For SrTiO$_3$, $c/a<1$, indicating tensile stress resulting from the larger BaZrO$_3$ rather than compression from the smaller LaAlO$_3$. The (110), (200), and (220) peaks are measured in a glancing-incidence geometry.

They are therefore not affected by broadening from finite layer thickness, leaving peak broadening due to finite in-plane grain size and stress inhomogeneity. Noting that the (220) peak is twice as broad as the (110), we can eliminate small-grain-size effects as a possible cause of line broadening, leaving a stress inhomogeneity of 1.8% full width at half maximum (FWHM). This indicates that the material near the interface may be under more strain than the middle of each layer.

For the samples with smaller periodicity (7/7 and 15/15), it was impossible to determine the in-plane and out-of-plane lattice parameters of the constituents independently. We can, however, safely assume that strain values obtained for the 20/20 structure represent a lower limit for the actual values present in the 7/7 and 15/15 structures.

From the data in Table I, the strain in each of the layers can be obtained. First, the intrinsic relaxed (cubic) lattice parameter of the SrTiO$_3$ and BaZrO$_3$ layers is calculated as

$$\hat{a} = \frac{(1-\nu)c + 2\nu a}{1+\nu},$$

where ν is Poisson's ratio. For an incompressible solid, $\nu = 0.5$; for bulk SrTiO$_3$, $\nu = 0.232$ (Ref. 17). The Poisson's ratios for thin films of SrTiO$_3$ and BaZrO$_3$ are not known: however, the in-plane strain $\varepsilon_{xx} = (a-\hat{a})/\hat{a}$ and the out-of-plane (or normal) strain $\varepsilon_{zz} = (c-\hat{a})/\hat{a}$ can be calculated for different values of ν and are found to be in the range of a fraction of a percent, as shown in Table I.

Not surprisingly, the films' intrinsic lattice parameter differs from that of the bulk value, as often observed for PLD-grown films due to a high density of point defects.

For dielectric measurements, interdigital (coplanar) Au/Cr electrode structures were deposited onto the film surfaces and the measurements were performed at 10 kHz. The finger spacing of these electrodes was 10 μm; thus, a bias voltage of 1 V corresponds to an electric field of 1 kV/cm. Measurements were performed either at room temperature or by immersing the entire structure in liquid nitrogen.

Figure 2 shows room-temperature dielectric data for various structures. The data in (a) and (b) are obtained for reference films of BaZrO$_3$ and SrTiO$_3$. As expected, little variation is observed in the capacitance (and thus the dielectric constant) as a function of applied dc voltage. The superlattices, in contrast, exhibit an interesting electric-field depen-

TABLE I. Observed lattice parameters of SrTiO$_3$ and BaZrO$_3$ in a (20/20) superlattice on LaAlO$_3$. The intrinsic film lattice parameter (relaxed cell volume) and the strain values are given for the bulk SrTiO$_3$ Poisson's ratio ($\nu = 0.232$) and for the limiting case of an incompressible solid ($\nu = 0.5$).

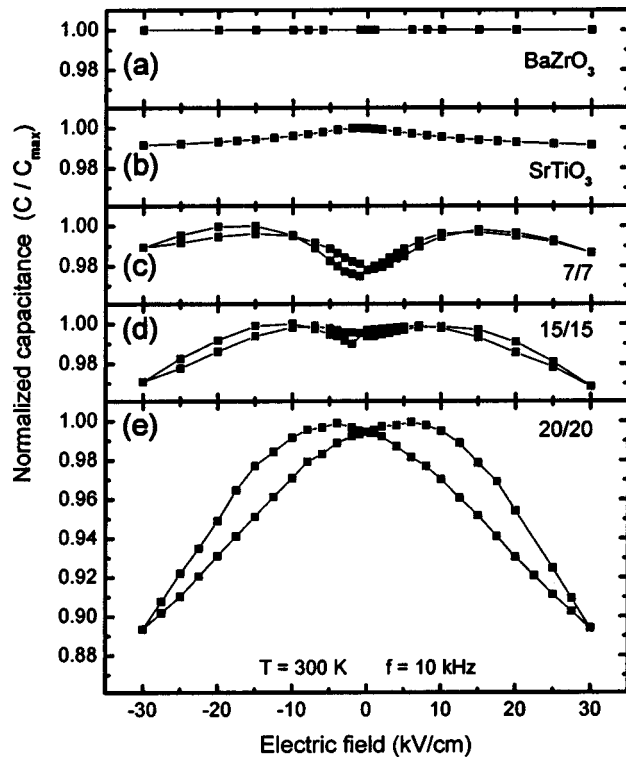|	Bulk a_0 (Å)	Film in-plane a (Å)	Film normal c (Å)	Intrinsic (cubic) film lattice para. $\hat{a}$	In-plane strain $\varepsilon_{xx} = (a-\hat{a})/\hat{a}$	Normal strain $\varepsilon_{zz} = (c-\hat{a})/\hat{a}$
SrTiO$_3$	3.905	3.955	3.918	3.943 ($\nu = .232$)	5.9×10^{-3} ($\nu = .232$)	-3.5×10^{-3} ($\nu = .232$)
				3.932 ($\nu = .5$)	3.1×10^{-3} ($\nu = .5$)	-6.2×10^{-3} ($\nu = .5$)
BaZrO$_3$	4.193	4.161	4.212	4.178 ($\nu = .232$)	-7.6×10^{-3} ($\nu = .232$)	4.6×10^{-3} ($\nu = .232$)
				4.193 ($\nu = .5$)	-4.1×10^{-3} ($\nu = .5$)	8.2×10^{-3} ($\nu = .5$)
LaAlO$_3$	3.788					

FIG. 2. Capacitance-voltage curves obtained using coplanar (interdigital) electrodes on various films on LaAlO$_3$ substrates at room temperature. (a) and (b) show the data for single-reference films of BaZrO$_3$ and SrTiO$_3$, respectively. In (c), (d), and (e), the data are presented for superlattices in which the BaZrO$_3$ and SrTiO$_3$ are 7, 15, and 20 unit cells thick, respectively. Total film thickness for all samples is 500 nm.
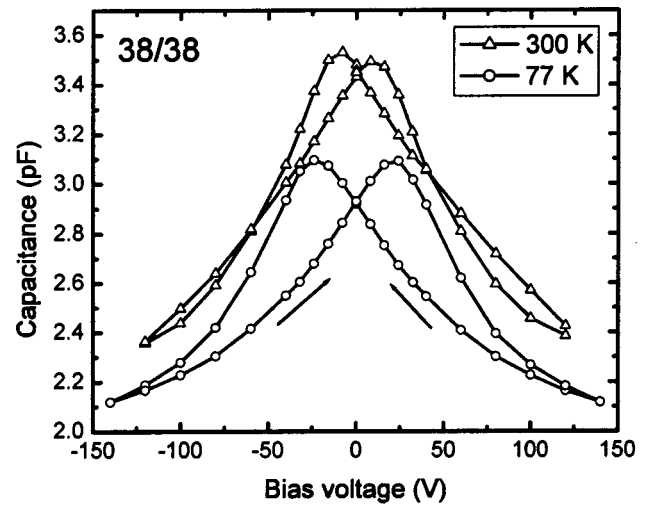

FIG. 3. Capacitance-voltage curves for a superlattice consisting of a periodic stacking of 38-unit-cell-thick layers of BaZrO$_3$ and SrTiO$_3$, measured at room temperature and in liquid nitrogen.

dence. Clearly, their behavior cannot be understood as a simple combination of the BaZrO$_3$ and SrTiO$_3$ properties, despite the fact that the in-plane measurement geometry would allow us to view the sample as a parallel combination of individual BaZrO$_3$ and SrTiO$_3$ layers. For the samples with the smallest periodicity (but with the same total sample thickness of 500 nm), the capacitance curves exhibit a local minimum at 0 kV/cm and two symmetrically placed maxima at a value that depends on the periodicity. For larger structures, such as shown in Fig. 2(e) (and also in Fig. 3: see below), a conventional (hysteretic) butterfly loop is observed. This type of curve is typically associated with ferroelectric structures. Note that here, however, neither of the two constituent materials of the superlattice is independently ferroelectric.

Figure 3 shows the capacitance versus voltage data for a 500-nm-thick film consisting of 16 pairs of SrTiO$_3$ and BaZrO$_3$, each layer being approximately 38 unit cells thick. Ferroelectric-type behavior is observed at both room temperature and 77 K.

The temperature dependence of the out-of-plane film lattice parameter was recorded from room temperature to 650 °C by x-ray diffraction (data not shown). Quite surprisingly, no anomaly is observed: i.e., the thermal expansion is linear over the entire range with a scatter of about 4 $\times 10^{-5}$. Thus, if a structural transition were present in this

temperature range [similar to our earlier work on KTaO$_3$/KNbO$_3$ (Ref. 6)], it would clearly be detected. It is important to point out, however, that the $(c-a)/a$ distortions in KTaO$_3$/KNbO$_3$ change by only about 30% at the transition and that the distortion observed here [$(c-a)/a \approx -9 \times 10^{-3}$] is comparable in magnitude to that observed in KTaO$_3$/KNbO$_3$ even in the high-temperature phase [$(c-a)/a \approx 6 \times 10^{-3}$].

Capacitance versus voltage [$C(V)$] curves are, by definition, the derivative (with respect to the electric field) of polarization versus field [$P(E)$] loops (in our case with the dc field swept at a very low rate of about 10^{-2} Hz, but the derivative taken at 10 kHz). Therefore, a single hysteresis loop [in $P(E)$] yields the traces as observed in our 20/20 and 38/38 structures. Antiferroelectricity or antiferroelectric dipole ordering between polar layers[18] is reflected by double hysteresis loops in $P(E)$ and, thus, by two maxima in the $C(V)$ curves (with a minimum at $V=0$), as observed in our 7/7 and 15/15 structures.

While our results by themselves may be insufficient to demonstrate ferroelectricity or antiferroelectricity (for example, the electrode geometry is inappropriate for recording polarization hysteresis loops), the observation of similar dipole patterns in BaTiO$_3$/SrTiO$_3$ and KTaO$_3$/KNbO$_3$ superlattices strongly supports such an interpretation. Our data are thus fully consistent with a picture of polar (ferroelectric) ordering within the SrTiO$_3$ and/or BaZrO$_3$ layers and a long-range (interlayer) polar order of antiferroelectric nature for spacing and thickness of 15 or fewer unit cells. For larger layer spacing and thickness, these ferroelectric slabs either show no long-range correlation or order ferroelectrically.

Antiferroelectric ordering between individual ferroelectric layers in a superlattice may be understood from energy arguments. In fact, the long-range nature of electric dipolar interaction leads to a large energy associated with long-range ferroelectric ordering. In ferroelectric crystals, where the ordering is mediated via elastic (short-range) interactions, domain formation reduces the energy associated with the dipo-

lar long-range interactions. The energy associated with the formation of domain walls determines the size of domains. Just as in the case of ferromagnetic films,[19] the equilibrium domain size in a ferroelectric layer scales as $D \propto \sqrt{t}$ and thus becomes larger than the film thickness below a critical value.[6] At this point, the equilibrium configuration is no longer determined by the properties of the individual layers in a superlattice, but by the total material within a domain. If the material has a structure that elastically allows for the formation of antiferroelectric ordering—as is the case in superlattices—antiferroelectric ordering will be favorable for certain values of elastic and dipolar interaction strengths.

The question remains, however, where the polarization resides. There are three obvious possibilities: either $SrTiO_3$ or $BaZrO_3$ could be ferroelectric under these strained conditions or the interface (and possibly an interdiffusion layer) could be responsible for the behavior. In fact, Ba diffusion into $SrTiO_3$ would render this material ferroelectric, but much more than 50% Ba needs to be substituted for Sr in order to achieve room-temperature ferroelectricity, even if it is assumed that Zr does not substitute for Ti. More importantly, however, in our previous work on superlattices of $SrTiO_3$ and $BaTiO_3$ (Ref. 20), where the same type of diffusion would be expected, we have observed distinctively different behavior between 4/4 superlattices and alloys. This indicates that under the growth conditions used here, interdiffusion—if it occurs—is restricted to a length scale of less than 4 unit cells. Ferroelectric-type behavior in the present $SrTiO_3 / BaZrO_3$ superlattices, however, is clearly apparent in structures with periodicities 10 times larger. We can therefore rule out interdiffusion as the dominating factor.

Consistent with the above-mentioned work on $LaAlO_3 / SrTiO_3$ structures, strain-induced room-temperature ferroelectricity in $SrTiO_3$ appears to be most likely. In fact, the earlier work on single-crystal materials[13,14] has shown that low-temperature ferroelectricity occurs in uniaxially stressed $SrTiO_3$. In this situation, the lattice distortion is of the same type as in this work: i.e., the unit cell dimensions are reduced in one direction and extended in the other two. Data for the actual distortions in the bulk experiments are not available, but an estimation can be made using published values of the elastic moduli ($c_{11} = 2.95 \times 10^{11}$ N/m^2 and $c_{12} = 1.15 \times 10^{11}$ N/m^2 at 30 K (Ref. 21)). For the highest stress investigated, $\sigma = 4 \times 10^8$ N/m^2 (for which a ferroelectric transition temperature $T_c \approx 30$ K was observed), these values yield $\Delta a/a \approx 4.9 \times 10^{-4}$ and $\Delta c/c \approx -1.7 \times 10^{-3}$. The fact that the distortions in our films are significantly larger supports the interpretation of a strain-induced ferroelectric phase in $SrTiO_3$ at room temperature. It appears, however, that much less strain is required in this symmetric environment to drive $SrTiO_3$ into a ferroelectric state than the value of 1.5×10^{-2} calculated for $SrTiO_3$ films with a free surface.[15]

To conclude, $SrTiO_3 / BaZrO_3$ superlattices exhibit dielectric properties that are very different from what would be expected based on reference data on $SrTiO_3$ and $BaZrO_3$ films. Strain-induced room-temperature ferroelectricity in $SrTiO_3$ and spacing-dependent coupling between the layers are proposed as mechanisms leading to this behavior. For large superlattice periodicities (20/20 and 38/38 structures), these ferroelectric layers appear to act as independent ferroelectric slabs or exhibit long-range ferroelectric ordering. For smaller periodicities (7/7 and 15/15), antiferroelectric coupling between these polar layers is observed, consistent with energy considerations for long-range electrostatic interactions and domain formation.

---

*Currently at Intel Massachusetts Inc., Hudson, MA 01749, USA.

[1] H. Tabata, H. Tanaka, and T. Kawai, Appl. Phys. Lett. **65**, 1970 (1994).

[2] J. C. Jang, X. Q. Pan, W. Tian, C. D. Theis, and D. G. Schlom, Appl. Phys. Lett. **74**, 2851 (1999).

[3] H.-M. Christen, L. A. Boatner, J. D. Budai, M. F. Chisholm, L. A. Gea, P. J. Marrero, and D. P. Norton, Appl. Phys. Lett. **68**, 1488 (1996).

[4] D. O'Neill, R. M. Bowman, and J. M. Gregg, Appl. Phys. Lett. **77**, 1520 (2000).

[5] J. B. Neaton and K. M. Rabe, Appl. Phys. Lett. **82**, 1586 (2003).

[6] H.-M. Christen, E. D. Specht, D. P. Norton, M. F. Chisholm, and L. A. Boatner, Appl. Phys. Lett. **72**, 2535 (1998), E. D. Specht, H.-M. Christen, D. P. Norton, and L. A. Boatner, Phys. Rev. Lett. **80**, 4317 (1998).

[7] M. Sepliarsky, S. R. Phillpot, M. G. Stachiotti, and R. L. Migoni, J. Appl. Phys. **91**, 3165 (2002), M. Sepliarsky, S. R. Phillpot, D. Wolf, M. G. Stachiotti, and R. L. Migoni, Phys. Rev. B **64**, 060101(R) (2002).

[8] H.-M. Christen, K. S. Harshavardhan, M. F. Chisholm, E. D. Specht, J. D. Budai, D. P. Norton, L. A. Boatner, and I. J. Pickering, J. Electroceram. **4**, 279 (2000).

[9] J. Sigman, D. P. Norton, H. M. Christen, P. H. Fleming, and L. A. Boatner, Phys. Rev. Lett. **88**, 097601 (2002).

[10] G. A. Samara and A. A. Giardini, Phys. Rev. **140**, A954 (1965).

[11] G. A. Samara, Phys. Rev. **151**, 378 (1966).

[12] T. Schimizu, Solid State Commun. **102**, 523 (1997).

[13] Y. Fujii, H. Uwe, and T. Sakudo, J. Phys. Soc. Jpn. **56**, 1940 (1987).

[14] C. Totsuji and T. Matsubara, J. Phys. Soc. Jpn. **60**, 3549 (1991).

[15] N. A. Pertsev, A. K. Tagantsev, and N. Setter, Phys. Rev. B **61**, R825 (2000); **65**, 219901(E) (2002).

[16] A. Q. Jiang, J. F. Scott, H. Lu, and Z. Chen, J. Appl. Phys. **93**, 1180 (2003).

[17] H. Ledbetter, M. Lei, and S. Kim, Phase Transitions **23**, 61 (1990).

[18] K.-H. Chew, L.-H. Ong, J. Osman, and D. R. Tilley, Appl. Phys. Lett. **77**, 2755 (2000).

[19] C. Kittel, Phys. Rev. **70**, 965 (1946).

[20] H.-M. Christen, L. A. Knauss, and K. S. Harshavardhan, Mater. Sci. Eng., B **56**, 200 (1998).

[21] W. Rehwald, Solid State Commun. **8**, 1483 (1970).